Ultrafast photogeneration mechanisms of triplet states in *para*-hexaphenyl

C. Zenz
Istituto Nazionale per la Fisica della Materia, Istituto di Matematica e Fisica, Università di Sassari, I-07100, Sassari, Italy and Institut für Festkörperphysik, Technische Universität Graz, A-8010 Graz, Austria

G. Cerullo
Istituto Nazionale per la Fisica della Materia, CEQSE-CNR, Dipartimento di Fisica, Politecnico di Milano, I-20133 Milano, Italy

G. Lanzani
Istituto Nazionale per la Fisica della Materia, Istituto di Matematica e Fisica, Università di Sassari, I-07100, Sassari, Italy

W. Graupner
Institut für Festkörperphysik, Technische Universität Graz, A-8010 Graz, Austria and Department of Physics, Virginia Polytechnic Institute and State University, Blacksburg, Virginia 24061-0435

F. Meghdadi and G. Leising
Institut für Festkörperphysik, Technische Universität Graz, A-8010 Graz, Austria

S. De Silvestri
Istituto Nazionale per la Fisica della Materia, CEQSE-CNR, Dipartimento di Fisica, Politecnico di Milano, I-20133 Milano, Italy

(Received 9 February 1999)

We present femtosecond pump-probe measurements, both conventional and electric field-assisted, on organic light-emitting devices based on *para*-hexaphenyl. The dominant triplet exciton generation mechanism is assigned to nongeminate bimolecular recombination of photogenerated, spin-$\frac{1}{2}$ polarons. This process is active within a few hundred femtoseconds after photoexcitation and involves about 20% of the initially excited states. At higher photoexcitation densities, we observe an additional triplet generation mechanism, which occurs in the 10-ps time domain, due to fusion of singlet excitons and subsequent fission into correlated triplet pairs. The latter decay on the 10^2-ps time scale by geminate recombination. [S0163-1829(99)01721-X]

I. INTRODUCTION

Organic π-conjugated molecules are very attractive materials for optoelectronic devices such as organic light-emitting diodes[1–4] (OLED's), light-emitting electrochemical cells,[5] photodiodes, and solar cells.[6] Among them, size-controlled oligomers can be regarded as model compounds for studying fundamental properties of π electrons in longer chain polymers. Light absorption in such materials results in the generation of intrachain electron-hole pairs, called excitons.[7] Dissociation of excitons is the dominant mechanism of charge-carrier (polaron) generation following photoexcitation. This process, which can be enhanced by applying an external electric field, is relevant for photovoltaic applications. The recombination of oppositely charged polarons into luminescent singlet excitons or nonradiative triplet excitons is one of the processes that govern the efficiency of OLED's. For this reason, studying the dissociation and recombination mechanisms is of fundamental importance both for applications and basic understanding.

In this work we present ultrafast pump/probe experiments performed on OLED structures consisting of aluminum/*para*-hexaphenyl (PHP)/indium tin oxide (ITO). PHP can be considered as a model substance for phenylene-based materials[8] and is used to build stable blue-emitting OLED's.[2–4,9] Due to its well-defined conjugation length and chemical structure, PHP exhibits well-resolved photoinduced absorption (PA) features that can be assigned to polaron-, triplet-, and singlet-state absorption. This allows us to optically address the exciton dissociation and polaron recombination dynamics in a real device structure with femtosecond time resolution. By using both conventional and field-assisted pump-probe techniques, we identify a fast nonconventional triplet exciton generation mechanism consisting of two steps: (i) singlet exciton dissociation into polarons and (ii) nongeminate bimolecular recombination of the polarons following the spin statistics. At high-excitation densities, an additional fast triplet exciton generation mechanism is observed, which is attributed to singlet exciton fusion and subsequent fission into correlated triplet pairs.

II. EXPERIMENT

Homogeneous, polycrystalline layers of highly purified PHP with a thickness of about 200 nm were evaporated onto ITO-covered glass substrates. Subsequently, an aluminum cathode was evaporated onto the PHP layer to obtain a single-layer OLED structure.

The laser source was a Ti:sapphire laser system with chirped-pulse amplification, which provided 140-fs pulses at 780 nm and 700-μJ energy at a repetition rate of 1 kHz. The excitation pulses at 390 nm were generated by second har-

monic of the fundamental beam in a 1-mm-thick LiB_3O_5 crystal. The pump beam was focused to a spot size of 80 μm, so the excitation energy density could be varied between 0.3 and 12 mJ/cm^2 per pulse. Conventional pump-probe experiments were carried out in the visible and near-infrared spectral range using the white-light supercontinuum generated in a thin sapphire plate.[10] Mirrors were used to collect the supercontinuum pulse and to focus it onto the sample in order to minimize frequency chirp effects. During the experiments the sample was kept in vacuum at room temperature.

The following measurements were carried out: (i) The whole white-light pulse was spectrally analyzed after traveling through the sample using a spectrometer and a silicon diode array. Transmission difference spectra are plotted as $\Delta T/T$, where ΔT is the pump-induced transmission change, obtained by subtracting pump-on and pump-off data, and T is the sample transmission. In the small signal limit $\Delta T/T \cong \Delta\alpha d$, where $\Delta\alpha$ is the absorbance change and d is the sample thickness (for very thick samples d is replaced by the pump penetration depth). Thus, $\Delta T/T$ is proportional to the excited-state population N, since $\Delta\alpha = \sigma N$, with σ the absorption cross section. $\Delta T > 0$ is associated to photobleaching (PB) or stimulated emission (SE), $\Delta T < 0$ to PA. Averaging over about 10^2 data acquisitions provides a sensitivity of about 10^{-3} in $\Delta T/T$; due to the small frequency chirp of the white-light pulse the overall time resolution in this experiment is 500 fs. (ii) The evolution in time of the ΔT signal is measured in a narrow spectral window of 10 nm using interference filters placed in front of the detector. In this case we use a preamplified photodiode and standard lock-in technique. This allows a higher sensitivity, of about 10^{-4} in $\Delta T/T$ and a better time resolution, which is limited by the experimental cross correlation to about 200 fs. In both experiments the pump and probe beams were linearly polarized, parallel to each other.

In electric field-assisted pump-probe experiments the pump and probe beams pass the glass, ITO, and polymer to be reflected by the aluminum. With the unbiased LED, we measured conventional transient pump/probe spectra, as previously described. With the device biased we measure the total dynamics in presence of the electric field, $(\Delta T/T)_F$. In order to detect small field-induced changes of ΔT, we apply a modulated voltage to the device and reference our detection to the field modulation (MF) frequency.[11] In this way we detect only field-induced changes[12] in the $\Delta T/T$ spectra, which we call $(\Delta T/T)_{\mathrm{MF}}$. Following our nomenclature, $(\Delta T/T)_{\mathrm{MF}} = (\Delta T/T)_F - \Delta T/T$. Note that the sign of $(\Delta T/T)_{\mathrm{MF}}$ at a given probe wavelength does not necessarily match the sign of $\Delta T/T$. For example, for PB or SE, $(\Delta T/T)_{\mathrm{MF}} > 0$ corresponds to a field-induced increase of the species responsible for the signal, while $(\Delta T/T)_{\mathrm{MF}} < 0$ corresponds to a field-induced quenching of the species; the contrary holds for PA.

Assuming a macroscopic average charge-carrier mobility of 10^{-3} cm^2/V s, we estimated that the characteristic time for the charges to travel to the electrodes under the maximum applied field of 1 MV/cm is 20 ns for a 200-nm-thick device. Hence, any dynamic effects caused by the movement of the charge carriers are much slower than the time scale of our measurement and can be neglected. Different phenomena can be identified looking at their peculiar time behavior. In general, $(\Delta T/T)_{\mathrm{MF}} = \Delta(\sigma N) = \Delta\sigma N + \sigma\Delta N$. $\Delta\sigma$ includes electric-field effects on the transition oscillator strength σ and Stark shifts of the molecular levels that are expected to be instantaneous.[11] Noninstantaneous ΔT_{MF} signals are ascribed to field-induced changes (ΔN) in the population density of the photogenerated species.

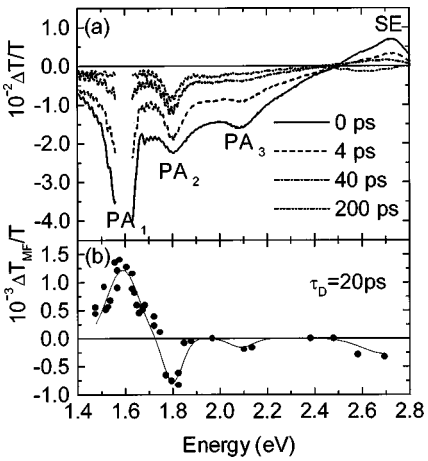

FIG. 1. (a) Conventional transient pump/probe spectra of the polycrystalline PHP film for different pump-probe delays, measured in an OLED structure. (b) The field-induced $(\Delta T/T)_{\mathrm{MF}}$ spectrum of PHP films for pump-probe delay of 20 ps and an applied-reverse bias of 16 V. Data points are obtained using a monochromator or interference filters. The solid line is a guide to the eye.

III. RESULTS AND DISCUSSION

A. Conventional pump-probe spectroscopy

Figure 1(a) shows conventional transmission difference spectra at room temperature for different pump-probe delays (τ_D). We observe a positive ΔT band for probing energies higher than 2.5 eV, peaking at about 2.7 eV. For lower probing energies, we observe three PA features peaking at 1.59 eV (PA_1), 1.8 eV (PA_2), and 2.09 eV (PA_3), respectively. Different decay kinetics, excitation intensity dependence, and field-induced changes indicate that PA_1, PA_2, and PA_3 have different origins.

We attribute the positive ΔT band at 2.7 eV to SE of the $S_1 \rightarrow S_0$ singlet exciton transition since strong photoluminescence in this region is observed while no significant ground-state absorption is measured.[13] The dynamics of PA_1 is depicted in Fig. 2(a) for an excitation energy of 42 nJ (corresponding to an approximate excitation density of 2×10^{19} cm^{-3}). Since it coincides with the dynamics of SE, it is straightforward to assign PA_1 to optical absorption from the lowest-excited singlet state S_1 to higher-lying states ($S_1 \rightarrow S_n$), in agreement with previous results.[13] Note that PA_1 is energetically positioned nearer to the fundamental frequency of the laser system. Therefore, we probe the temporal evolution of PA_1 not at the peak position, but at its lower energy side, at 1.51 eV. The decay at this pump-pulse energy matches a stretched exponential function $PA_1(t) \propto \exp[(-t/\tau)^{\alpha}]$ with $\tau = 75$ ps and $\alpha = 0.5$, according to monomolecular recombination in a disordered material.[14] In agreement with doping-induced spectra of hexaphenyl[15] and theoretical calculations[16] that predict two absorption bands at

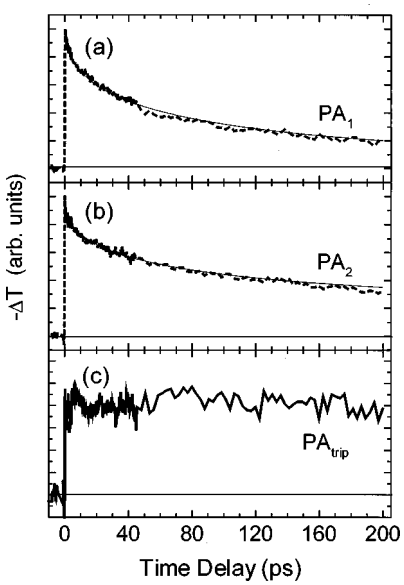

FIG. 2. (a) Normalized time traces of the PA_1 absorption band at 1.59 eV for a pump-pulse energy of 42 nJ. (b) Normalized time traces of PA_2 at a probe energy of 1.8 eV for a pump-pulse energy of 42 nJ (dashed lines). Solid lines are fitted. (c) PA_{trip} due to actual triplet population (see text).

0.7 and 1.95 eV for singly charged polarons, we assign PA_3 at 2.09 eV to photoinduced polaron absorption. PA_2 at 1.8 eV is the only persistent feature at 400 ps [Fig. 1(a)]. This band is assigned to triplet-triplet transitions ($T_1 \rightarrow T_n$) based on cw-PA measurements.[17] For short delays, the high-energy tail of PA_1 is superimposed on PA_2; therefore the actual dynamics of PA_2 can be separated by using the *known* time dependence of PA. The measured dynamics at 1.8 eV for low pump-pulse energies (<42 nJ) [Fig. 2(b)] can be reproduced by a stretched exponential with the *same parameters* as for PA_1 plus a plateau. In Fig. 2(c) we plotted the difference, after proper normalization, of the ΔT traces at 1.59 and 1.8 eV, which shows the PA_2 dynamics assigned to triplet population. The results suggest that the formation of a long-living triplet state occurs *within* the pump-pulse duration ($\tau_p < 200$ fs), consistently with the $\Delta T/T$ spectrum for $\tau_D = 0$ ps [Fig. 1(a)], which shows already the triplet feature. This observation is in contrast to the conventional mechanism of intersystem crossing (ISC) observed in molecular solids due to spin wave-function mixing. In this case, the triplet population should show a build-up time that corresponds to the singlet decay. In addition, a simple argument proves that a sizable triplet population cannot be reached within 200 fs via spin-orbit coupling ISC. The upper limit for the ISC rate (τ_{ISC}^{-1}) is obtained considering triplet generation as the only nonradiative decay mechanism. The photoluminescence quantum yield of PHP is about 30%,[13] so if the remaining 70% of the excitation goes into the triplet state and considering a singlet lifetime of about 200 ps, as determined approximating the nonexponential decay [Fig. 2(a)], τ_{ISC} can be estimated to be 290 ps. After 500 fs the triplet population (n_T) formed at such rate is then $n_T(500\,\text{fs}) = 2 \times 10^{-3} n_S(0)$, where $n_S(0)$ is the initial singlet population. Assuming a cross section for triplet-triplet absorption of the same order of magnitude as that for the singlet transition, the triplet PA at $\tau_D = 500$ fs would be three orders of magnitude below our sensitivity and could not be detected.

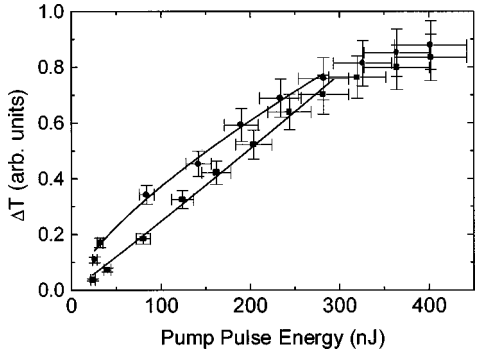

FIG. 3. Excitation density dependence for PA_1 at zero time delay (circles), and PA_2 at 400-ps time delay (crosses). The solid lines are fitted.

Also, we can exclude singlet fission[18] to be the dominant triplet formation mechanism in PHP for the following reasons: (i) fission results into correlated pairs that have a high probability of mutual annihilation, i.e., shorter lifetime, usually in the ps time domain.[18] (ii) Fission requires the excitation photon energy be larger than twice the lowest triplet-state energy $E(T_1)$. Based on data for methyl substituted ladder-type poly(*para*-phenylene), where the onset for fission is observed for excitation photon energies at 3.2 eV [$E(T_1) \approx 1.6$ eV],[19] we can estimate that the lowest-lying triplet is located higher than 1.6 eV in PHP due to the shorter effective conjugation length. Thus, the excitation energy used in our experiments (3.18 eV) is too small to explain the observed triplet yield. (iii) Singlet fission from a higher excited state S_1^* that is populated by a second-order process, such as two-photon absorption or two-step absorption, is nonlinear with respect to the intensity of the light excitation.[20] The excitation intensity dependence of PA_1, monitored at $\tau_D = 0$ ps, and PA_2, monitored at 400 ps, is plotted in Fig. 3. It will be clear later that PA_2 at such a delay is only due to the long-lived triplet population, associated with the ultrafast generation process. For low-medium pump-pulse energies PA_2 shows a linear excitation dependence, whereas PA_1 grows sublinearly (fitting in the figure are I^x, with $x \approx 0.7$ from 40 to 300 nJ for PA_1, and with $x \approx 1.0$ for PA_2). This behavior is consistent with the model proposed in the following section.

B. Electric field-assisted pump-probe spectroscopy

To clearly identify the triplet formation mechanism in PHP, we performed field-assisted pump-probe experiments. The reverse biasing of the LED ensures negligible injection from the electrodes, so that exciton-carrier interactions can be disregarded.[21] Figure 1(b) shows a $(\Delta T)_{MF}$ spectrum obtained for a delay of 20 ps and an applied reverse bias of 16 V. We observe a transient decrease of SE [negative $(\Delta T/T)_{MF}$ signal] and PA_1 [positive $(\Delta T/T)_{MF}$ signal] that can be explained by field-induced dissociation of the singlet exciton population, similar to the effect under steady-state condition.[22–25] We emphasize that the *correlated decrease of SE and* PA_1 is a further indication for the assignment of PA_1 to singlet exciton transitions, whereas *both* PA_2 *and* PA_3 are

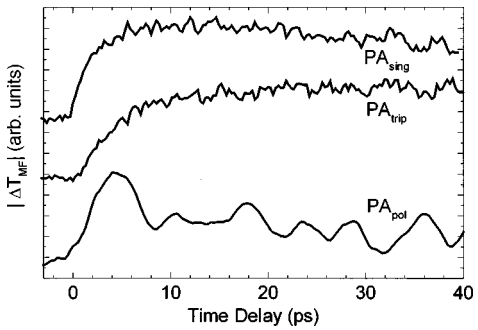

FIG. 4. Normalized field-induced quenching of the singlet absorption (PA_{sing}) at 1.59 eV, increase of the triplet absorption (PA_{trip}) at 1.8 eV, and increase of the polaron absorption (PA_{pol}) at 2.09 eV for an applied reverse bias of 16 V and a pump-pulse energy of 160 nJ. Traces are vertically displaced for clarity.

increased by the applied field [negative $(\Delta T/T)_{MF}$ signal], indicating a corresponding increase of polaron and triplet population. The normalized field-induced changes of the populations are plotted in Fig. 4 vs pump-probe delay, after being corrected for the spectral overlap. The initial fast rise of the field-induced polaron population (PA_{pol}) is correlated to the singlet exciton (PA_{sing}) quenching within the noise level indicating a direct dissociation of singlets into polarons.[12] The field-induced triplet population (PA_{trip}) shows a much slower build-up dynamics, excluding a direct reaction from singlets to the triplets. Therefore, we propose a stepwise formation process: (1) breaking of hot excitons into spin-$\frac{1}{2}$ polarons; (2) nongeminate bimolecular recombination of polarons into triplet and singlet excitons with a ratio of 3:1 following the spin statistics. Within this model the field-induced triplet generation process is a bimolecular reaction that should show an excitation density dependence. This can be demonstrated by the experimental results reported in Fig. 5, showing $(\Delta T/T)_{MF}$ for the triplet exciton at different excitation densities: these results clearly indicate decrease of the field-induced triplet formation time upon increasing the excitation densities. From the dynamics we can extract a coefficient k for the bimolecular polaron recombination in the ps time domain ($k=4\times10^{-6}$ cm^3/s). Direct recombination of polarons implies a relation between k and the mobility μ, given by $k=[e/(\varepsilon_0\varepsilon_r)]\mu$, where e is the electron charge, ε_0 and ε_r are the vacuum and relative dielectric constants. Assuming $\varepsilon_r=4$, we obtain $\mu=8$ cm^2/V s, a value that can be observed in single crystalline organic materials.[26] However, it should be noted that this mobility is related to hot polarons within a nanocrystal of PHP, i.e., it is a value in a single crystal that is not affected by mesoscopic or macroscopic motion constrains. For this reason such mobility cannot be observed by conventional electrical or electro-optical techniques due to the polycrystalline texture of PHP films.

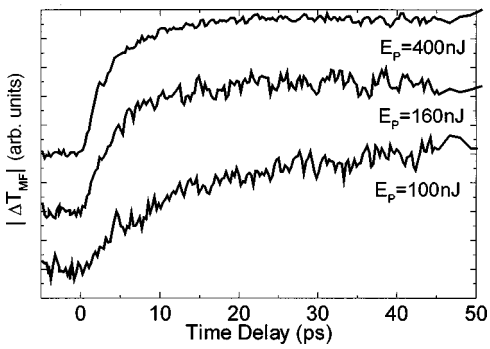

FIG. 5. Normalized field-induced buildup of the triplet absorption (PA_{trip}) at 1.8 eV for pump-pulse energies of 100, 160, and 400 nJ. Traces are vertically displaced for clarity.

We conjecture that this triplet formation mechanism is also active without an applied electric field. In this case, ultrafast dissociation of a fraction of the initial exciton population, possibly assisted by disorder[19] or caused by singlet exciton fusion,[27] instantaneously creates polarons at high density. Assuming an equal cross section for triplet and singlet absorption, a 20% yield of free charge carriers is sufficient to explain the magnitude of the observed zero-field triplet signal. The high density of photogenerated polarons gives rise to an ultrafast nongeminate recombination into triplet excitons, which is comparable to the experimental resolution of our setup. The situation is different in field-assisted pump-probe measurements. From the magnitude of the field-induced signal we deduce that less than 2% of the photoexcitations are affected by the applied field. As a consequence of the time-delayed generation of the charge carriers (see Fig. 4) and of their lower density, the recombination of polarons into triplet excitons can be time resolved. We emphasize again, that this bimolecular character of the triplet formation and the strong dependence on the polaron density is demonstrated by the experimental results shown in Fig. 5. The reported sublinear intensity dependence for PA_1 may indicate that the initial hot exciton dissociation is indeed a many-body effect, which becomes more effective at higher density.

C. High excitation density dynamics

A second mechanism for triplet generation in PHP becomes evident when the excitation density is increased. Time traces for pump-pulse energy of 400 nJ, corresponding to an estimated excitation density of 2×10^{20} cm^{-3} [see Fig. 6(a)] show faster PA_1 decay dynamics, which indicates bimolecular singlet annihilation[13] on the 10-ps time scale. Moreover, for these high pump-pulse energies the PA_2 dynamics can no longer be reproduced by the superposition of a plateau due to a long-living triplet population and PA_1. Fitting requires an additional short-living triplet population PA_{ST} that accounts for up to 20% of the signal. The extracted time behavior for PA_{ST} is plotted in Fig. 6(c). From this plot we see that PA_{ST} has a finite formation time, of about 10 ps, and decays in the 10^2-ps time domain, reflecting the dynamics of the additional generated triplet population.

Note, that the linear excitation density dependence reported in Fig. 3 is measured at a 400-ps time delay. Thus a contribution of the short-living triplet population can be neglected at this time delay.

The results reported so far can be rationalized considering two distinct triplet generation mechanisms: (i) a recombination of polarons, as discussed previously, and (ii) a mechanism occurring in the ps timescale at high excitation densities, generating *short-living triplets*. The observed fast decay is obviously in contrast with the metastable character of the

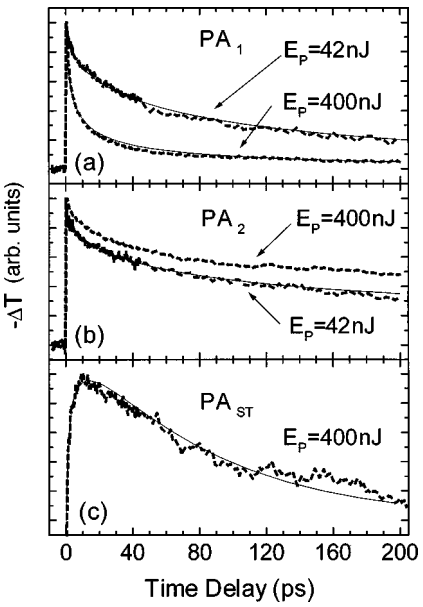

FIG. 6. (a) Normalized time traces of the PA_1 absorption band at 1.59 eV for different pump-pulse energies (dashed lines). (b) Normalized time traces of PA_2 at a probe energy of 1.8 eV for different pump-pulse energies (dashed lines). (c) PA due to the additional short-living triplet population Δn_T (PA_{ST}) (see text). The smooth curves are calculated according to the rate equations in the text.

triplet state, but can be explained by the presence of triplet pairs with correlated spins that decay due to internal geminate coalescence.[18] Since we observe that the additional triplet population is formed on the same time scale of singlet-singlet annihilation, we suggest the following reaction: $S_1+S_1\rightarrow S_x\rightarrow T_1+T_1$, i.e., singlet fusion with subsequent fission into correlated triplet pairs. To confirm this mechanism, we have tried to reproduce the experimental data by numerical integration of the following rate equations:

$$\frac{dn_S}{dt}=-\frac{\alpha}{\tau_S^{\alpha}}t^{\alpha-1}n_S-\gamma t^{-0.5}n_S^2, \tag{1}$$

$$\frac{d\Delta n_T}{dt}=\gamma t^{-0.5}n_S^2-\frac{\Delta n_T}{\tau_T}, \tag{2}$$

where n_S is the singlet exciton population, τ_S is the singlet exciton decay time, γ is the bimolecular recombination rate due to singlet annihilation, Δn_T is the fraction of the triplet exciton population generated by fission, and τ_T is the decay time of Δn_T. The first term on the right-hand side of Eq. (1) is the time-dependent recombination rate that yields the previously mentioned stretched-exponential behavior. The second term accounts for the bimolecular fusion-fission process.[28] Using the monomolecular decay parameters τ_S and α, as obtained from the fitting of PA_1 at low-pump energies, an initial excitation density of $3.5\times10^{19}\,\mathrm{cm}^{-3}$ and a recombination rate of $6.6\times10^{-15}\,\mathrm{cm}^3\,\mathrm{s}^{-1/2}$, we are able to reproduce the PA_1 and PA_2 dynamics for excitation densities within the investigated range with good agreement [Figs. 6(a) and 6(b)]. In particular, the formation and decay of the additional triplet population Δn_T formed by singlet fission can be well reproduced. The decay time constant, approximating the kinetics with a single exponential, is $\tau_T=75$ ps [Fig. 6(c)], and accounts for geminate recombination of the triplet pairs.

IV. CONCLUSIONS

In conclusion, we have performed transient pump and probe experiments on single layer PHP-OLED's with and without an applied external field. Singlet, triplet, and polaron absorption are identified, associated with PA bands at an energy of 1.59, 1.8, and 2.09 eV, respectively. Based on transient data with and without electric field, we identify two distinct triplet formation mechanisms in PHP. First, bimolecular recombination of photoinduced polarons gives rise to a long-living triplet population. Electric field-assisted pump-probe experiments allow us to directly probe this process, enhancing singlet exciton dissociation into polarons and thus increasing the nongeminate recombination into triplet excitons. Second, at high excitation densities we observe triplet generation due to fusion fission of singlet excitons into correlated triplet pairs, which decay in the 100-ps time domain.

The field-assisted experiments suggest a scenario of photoexcitation in PHP nanocrystals. The primary neutral intrachain state can dissociate during the first hundred femtoseconds into highly mobile spin-$\frac{1}{2}$ states that quickly recombine according to spin statistics. Some consideration on energetics should be done. The wave-function delocalization is not known in PHP. It can be estimated roughly by Stark-shifted polarizability of the excited state[11] to be 10 Å, i.e., of the same order of magnitude of the intermolecular distance (about 5 Å) in the crystal.[29] The initial excited state has only 0.2 eV excess energy with respect to the optical gap, but due to the close molecular packing in the crystal this energy can be enough to allow disorder-assisted dissociation into pairs and following polarons. Polaron-polaron interaction may thus occur among free, highly mobile polarons, or by polaron exchange among adjacent pairs. In the latter case the effective parameters of the interaction would be the recombination rate k, and not the mobility of the polarons. Triplets are favored by the low-energy position with respect to singlet, but also ''thermalized'' singlets should lie below the hot pair energy. This ultrashort living phase of the photoexcited material is unexpected in molecular semiconductors, and contradicts the general wisdom for Frenkel states. Note, however, that the final result, after dynamic state mixing, is again a distribution of neutral states. Thus, the quantum yield for free charge carriers is small.

ACKNOWLEDGMENTS

C.Z. gratefully acknowledges financial support through EC Contract No. FMRX-CT97-0106. F.M. was financially supported by SFB-Elektroaktive Stoffe. We thank V. Dyakonov for helpful discussions.

[1] J. H. Burroughes, D. D. C. Bradley, A. R. Brown, R. N. Marks, K. Mackay, R. H. Friend, P. L. Burn, A. Kraft, and A. B. Holmes, Nature (London) **347**, 539 (1990).
[2] W. Graupner, G. Grem, F. Meghdadi, Ch. Paar, G. Leising, U. Scherf, K. Müllen, W. Fischer, and F. Stelzer, Mol. Cryst. Liq. Crsyt. Sci. Technol., Sect. A **256**, 549 (1994).
[3] M. Era, T. Tsutsui, and S. Saito, Appl. Phys. Lett. **67**, 2436 (1995).
[4] S. Tasch, Ch. Brandstätter, F. Meghdadi, G. Leising, G. Froyer, and L. Athouel, Adv. Mater. **9**, 33 (1997).
[5] Q. Pei, G. Yu, Ch. Zhang, Y. Yang, and A. J. Heeger, Science **269**, 1086 (1995).
[6] N. S. Sariciftci, L. Smilowitz, A. J. Heeger, and F. Wudl, Science **258**, 1474 (1992).
[7] V. Dyakonov, G. Rösler, M. Schwoerer, and E. L. Frankevich, Phys. Rev. B **56**, 3852 (1997).
[8] J. Stampfl, S. Tasch, G. Leising, and U. Scherf, Synth. Met. **71**, 2125 (1995).
[9] G. Grem, G. Leditzky, B. Ullrich, and G. Leising, Adv. Mater. **4**, 36 (1992).
[10] G. Cerullo, S. Stagira, M. Nisoli, S. De Silvestri, G. Lanzani, G. Kranzelbinder, W. Graupner, and G. Leising, Phys. Rev. B **57**, 12 806 (1998).
[11] W. Graupner, G. Lanzani, G. Cerullo, C. Zenz, E. J. W. List, G. Leising, and S. De Silvestri, Synth. Met. (to be published).
[12] W. Graupner, G. Cerullo, G. Lanzani, M. Nisoli, E. J. W. List, G. Leising, and S. De Silvestri, Phys. Rev. Lett. **81**, 3259 (1998).
[13] A. Piaggi, G. Lanzani, G. Bongiovanni, A. Mura, W. Graupner, F. Meghdadi, G. Leising, and M. Nisoli, Phys. Rev. B **56**, 10 133 (1997).
[14] G. Lanzani, M. Nisoli, S. De Silvestri, and F. Abbate, Chem. Phys. Lett. **264**, 667 (1997).
[15] R. K. Khanna, Y. M. Jiang, B. Srinivas, C. B. Smithhart, and D. L. Wertz, Chem. Mater. **5**, 1792 (1993).
[16] E. Zojer, J. Cornil, G. Leising, and J. L. Brédas, Phys. Rev. B **59**, 7957 (1999).
[17] W. Graupner, F. Meghdadi, G. Leising, G. Lanzani, M. Nisoli, S. De Silvestri, W. Fischer, and F. Stelzer, Phys. Rev. B **56**, 10 128 (1997).
[18] B. Kraabel, D. Hulin, C. Aslangul, C. Lapersonne-Meyer, and M. Schott, Chem. Phys. **227**, 83 (1998).
[19] M. Wohlgenannt, W. Graupner, G. Leising, and Z. V. Vardeny, Phys. Rev. Lett. **82**, 3344 (1999).
[20] R. Katoh, M. Kotani, Y. Hirata, and T. Okada, Chem. Phys. Lett. **264**, 631 (1997).
[21] S. Barth, H. Bässler, H. Rost, and H. H. Hörhold, Phys. Rev. B **56**, 3844 (1997).
[22] R. Kersting, U. Lemmer, M. Deussen, H. J. Bakker, E. F. Mahrt, H. Kurz, V. I. Arkhipov, H. Bässler, and E. O. Göbel, Phys. Rev. Lett. **73**, 1440 (1994).
[23] U. Lemmer, S. Karg, M. Scheidler, M. Deussen, W. Rieß, B. Cleve, P. Thomas, H. Bässler, M. Schwoerer, and E. O. Göbel, Synth. Met. **67**, 169 (1994).
[24] G. E. O'Keefe, J. J. M. Halls, C. A. Walsh, G. J. Denton, R. H. Friend, and H. L. Anderson, Chem. Phys. Lett. **276**, 78 (1997).
[25] S. Tasch, G. Kranzelbinder, G. Leising, and U. Scherf, Phys. Rev. B **55**, 5079 (1997).
[26] *Numerical Data and Functional Relationships in Science and Technology*, edited by O. Madelung, Landolt-Börnstein, New Series, Group III, Vol. 17, pt. 1 (Springer, Berlin, 1985).
[27] A. D. Walser, I. Sokolik, R. Priestley, and R. Dorsinville, Appl. Phys. Lett. **69**, 1677 (1996).
[28] B. I. Greene and R. R. Millard, Phys. Rev. Lett. **55**, 1331 (1995).
[29] K. N. Baker, A. V. Fratini, T. Resch, H. C. Knachel, W. W. Adams, E. P. Sacci, and B. L. Farmer, Polymer **34**, 1571 (1993).